JACS
JOURNAL OF THE AMERICAN CHEMICAL SOCIETY
Article
pubs.acs.org/JACS

Efficient Electrocatalytic Water Oxidation at Neutral and High pH by Adventitious Nickel at Nanomolar Concentrations

Isolda Roger and Mark D. Symes*

WestCHEM, School of Chemistry, University of Glasgow, University Avenue, Glasgow, G12 8QQ, U.K.

Supporting Information

ABSTRACT: Electrolytic water oxidation using earth-abundant elements is a key challenge in the quest to develop cheap, large surface area arrays for solar-to-hydrogen conversion. There have been numerous studies in this area in recent years, but there remains an imperative to demonstrate that the current densities reported are indeed due to the species under consideration and not due to the presence of adventitious (yet possibly highly active) contaminants at low levels. Herein, we show that adventitious nickel at concentrations as low as 17 nM can act as a water oxidation catalyst in mildly basic aqueous solutions, achieving stable (tens of hours) current densities of 1 mA cm^{-2} at overpotentials as low as 540 mV at pH 9.2 and 400 mV at pH 13. This nickel was not added to the electrolysis baths deliberately, but it was found to be present in the electrolytes as an impurity by ICP-MS. The presence of nickel on anodes from extended-time bulk electrolysis experiments was confirmed by XPS. In showing that such low levels of nickel can perform water oxidation at overpotentials comparable to many recently reported water oxidation catalysts, this work serves to raise the burden of proof required of new materials in this field: contamination by adventitious metal ions at trace loadings must be excluded as a possible cause of any observed water oxidation activity.

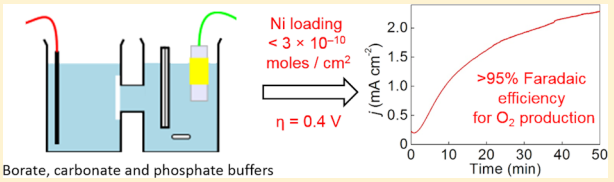

INTRODUCTION

There has been much interest recently in electrocatalytic and photocatalytic water splitting as routes toward storing intermittent renewably generated power (especially solar power) as chemical fuels, such as hydrogen.[1−3] Acid-regime proton-electrolyte membrane electrolyzers (PEMEs) have been proposed for this purpose, as they respond well to fluctuations in power inputs.[4] However, the most effective catalysts yet identified for PEMEs are based on very rare elements.[5] This presents a challenge for photodriven water splitting in particular, as the low photocurrents typically afforded by solar irradiation will require large electrode surface areas in order to produce useful amounts of fuel on practical time scales. Hence, if widespread solar-driven water splitting is to become a reality, then the loadings of any rare water-splitting catalysts must be lowered and/or less rare alternatives must be found.[6] Alkaline electrolysis represents a possible solution to the issues of catalyst scarcity (porous Ni and steel electrodes in commercial electrolyzers allow current densities of 0.5 A cm^{-2} to be achieved at ∼300 mV overpotential),[7] but there is also a need to move away from the extreme pH regimes characteristic of such traditional commercial devices (pH ∼0 for proton exchange membrane electrolyzers and pH >14 for alkaline electrolyzers),[4] because such corrosive conditions limit the types of photoelectrodes and cell components that can be used.[8,9]

Studies on heterogeneous water oxidation catalysts that operate under the mild pH conditions that are compatible with existing photoelectrodes have therefore focused largely on first-row transition metals due to their relatively high abundance in the Earth's crust. Some recent notable examples of such heterogeneous catalysts include cobalt oxides and oxyhydroxides,[10−18] nickel oxides,[19−24] manganese oxides,[25−33] copper oxides,[34−36] and mixed oxides of first-row transition metals.[37−44] Some of these potential catalysts have already been used in conjunction with light-harvesting substrates to produce photoanodes competent for light-driven water oxidation.[45−55] Meanwhile, catalysis with second- and third-row transition metals has been largely limited to compounds based on more scarce elements, such as rhodium,[56] ruthenium,[57] and iridium.[48,58−62]

A typical strategy that is adopted when assessing the efficacy of such heterogeneous catalysts is to obtain current density vs overpotential profiles and then to compare the overpotential required to reach some benchmark current density (often 1 mA cm^{-2} or 10 mA cm^{-2}) with that required to reach the same current density with other materials. Under basic conditions, an overpotential of between 0.33 and 0.5 V (to achieve a current density of 10 mA cm^{-2} for water oxidation) is considered as promising for solar-to-hydrogen applications.[63] However, this remains a somewhat challenging target, and many materials with overpotential requirements in excess of this 0.33−0.5 V window have been (and continue to be) reported. Perhaps on account of the difficulty of demonstrating stable and sustained heterogeneous water oxidation catalysis at such comparatively low overpotentials, many studies assume that the background activity for water oxidation must be negligible, and control

Received: August 3, 2015
Published: October 18, 2015

DOI: 10.1021/jacs.5b08139
J. Am. Chem. Soc. 2015, 137, 13980−13988

experiments may consist simply of a cyclic voltammogram in the absence of the material under investigation. However, such short-duration experiments may be insufficient to rule out the agency of trace metal impurities in any longer-term water oxidation catalysis observed with the proposed catalyst systems.

The issue of what the true catalyst for a given reaction actually is under a given set of conditions has been highlighted in seminal reviews by Widegren and Finke[64] and Crabtree.[65] The latter paper in particular describes the effect that impurities can have in catalytic reactions, stating, "The phenomenally low loadings of metal that can give high activity is a major hazard in this area." In recent years, the true nature of a range of catalysts with specific reference to water splitting has been explored,[66,67] with special attention paid to the role that low levels of simple Co(II) salts (formed from the degradation of higher nuclearity homogeneous species) could have in electrocatalytic water oxidation.[68−70] The effect that iron impurities have on nickel oxide water oxidation catalysts has also been reported.[40,71−75] In this context, establishing the cause of any unexpectedly high water oxidation activity—including the potential agency of trace impurities in this catalysis—remains vital for advancing the field.

Herein, we show that nickel at very low concentrations (17 nM, giving an electrode surface loading of less than 1 nmol per cm^2) constitutes a competent catalyst for water oxidation over the pH range 9.2−13, delivering stable current densities of 1 mA cm^{-2} at overpotentials of 540 mV at pH 9.2 and 400 mV at pH 13 for periods of several tens of hours. This nickel was *not* added to the electrolysis baths deliberately. Rather, it was present as a trace impurity in the supporting electrolyte salts (and possibly even in the ostensibly deionized water used to prepare the electrolytes), and its water oxidation activity only manifested after several minutes of anodic polarization in electrolysis experiments. Furthermore, at these low loadings, the nickel oxide catalyst layer on the anode was undetectable by eye or by SEM/EDX, and the presence of nickel was only evident by ICP-MS analysis of the electrolyte and by comparison of XPS spectra run in as-prepared and carefully washed electrolyte solutions. Although we cannot exclude the possibility that the nickel oxide deposits formed do not also contain traces of Fe,[71−73] we show that the concentration of nickel in the electrolyte solution is a critical determinant of the extent of water oxidation catalysis. The very low levels of nickel required to produce respectable and reproducible activities for electrochemical water oxidation serve to raise the bar when investigating the activity of heterogeneous water oxidation catalysts at neutral and basic pH: for other materials that display similar current densities at these overpotentials, it must be demonstrated that adventitious nickel contamination is not a cause of the observed activity.

RESULTS AND DISCUSSION

As part of our ongoing studies of electrocatalytic water oxidation using earth-abundant elements,[16] we had occasion to conduct control experiments in which a fluorine-doped tin oxide on glass (FTO) working electrode was poised at overpotentials of around 600 mV in a single-chamber electrolysis cell, along with a Pt wire counter electrode and an Ag/AgCl reference electrode. Under stirring in potassium borate buffer (0.5 M, pH 9.2), the current declined gently for the first few hundred seconds, much as expected. However, we were surprised to observe a subsequent steady rise in current, the onset of which typically occurred between 60 and 600 s after the beginning of the polarization, and which continued for several hours before reaching a plateau at between 1 and ∼4 mA cm^{-2} (see Figure 1). This phenomenon was found to be highly reproducible and could be observed on both FTO electrodes poised anodically in fresh solutions and FTO electrodes poised anodically in solutions that had previously displayed this behavior.

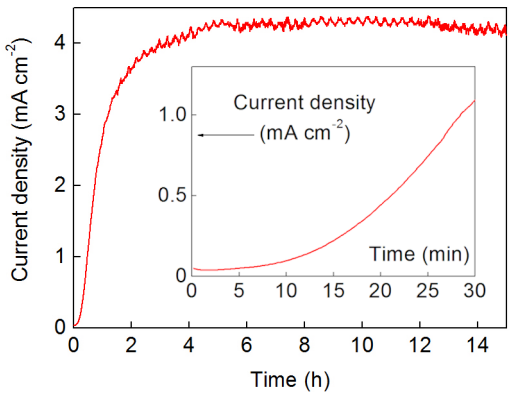

Figure 1. A bulk electrolysis experiment performed with a 1 cm^2 FTO working electrode, Ag/AgCl reference electrode, and a Pt wire counter electrode in 0.5 M potassium borate (pH 9.2) at room temperature. A single-chamber cell was used and the electrolyte was stirred throughout. A potential of 1.4 V vs NHE was maintained, and the data are not corrected for solution resistance (R = 31 Ω). Inset: An expansion of the first 30 min of the main panel, showing the steady rise of the current density after an initial lag phase.

Figure 1 shows that this high current was maintained for periods of over 10 h, and in some cases, current densities well in excess of 1 mA cm^{-2} were sustained for up to 72 h, showing no sign of decreasing. During this time, steady bubbling could be observed from the FTO anode, which appeared identical by eye to fresh FTO. In the absence, to our knowledge, of any previous reports of similar behavior for FTO without the addition of catalysts and intrigued by these large "control" currents (in many cases outperforming the substances we were trying to assess), we began a systematic study of these electrochemical processes in the hope of finding the cause of this activity.

Figure 2 compares Tafel plots obtained for FTO electrodes that had been polarized anodically in 0.5 M potassium borate buffer at 700 mV overpotential until the current density had reached a plateau with the behavior of fresh FTO electrodes that had not been subjected to prior anodization in this fashion. Preanodized electrodes displayed reproducible Tafel slopes of 57 mV (±2 mV) over nearly three decades of log current density, while nonanodized electrodes gave slopes in the region of 120 mV per decade at low current densities (less than 0.1 mA cm^{-2}).

We also compared cyclic voltammograms (CVs) of anodized and nonanodized (fresh) films in the presence of 1 mM ferricyanide in order to determine if there was any significant increase in the surface area of the electrode as a result of anodization. If the electrode surface area was increasing with prolonged anodization, then a larger reversible wave for the Fe(II)/Fe(III) redox couple should be evident for the anodized electrodes. As a control, CVs of nonanodized electrodes having a range of known geometric surface areas were first obtained, which allowed a linear relationship between electrode surface

DOI: 10.1021/jacs.5b08139
J. Am. Chem. Soc. 2015, 137, 13980−13988

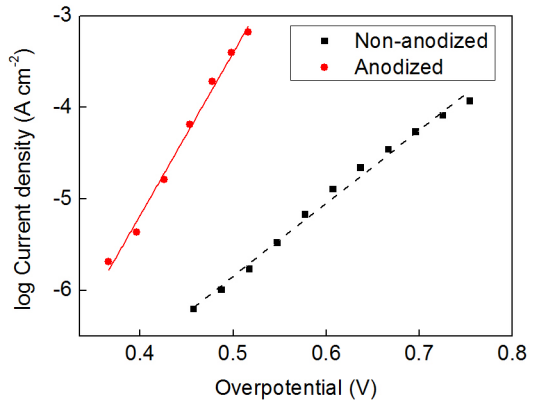

Figure 2. Representative Tafel plots of anodized (red line and circles) and nonanodized FTO films (black squares and dashed line) in 0.5 M potassium borate solution at pH 9.2. Anodization was conducted at 1.4 V vs NHE for 24 h [see the Supporting Information (SI) for details]. Overpotentials in the figure have been corrected for resistance.

area and peak current in the CV to be established (see Figure S1a,b, SI). Figures S2 and S3 (SI) then compare CVs taken before and after anodization at +1.0 V vs NHE for 24 h, during which time the current density rose to a steady 2.3 mA cm^{-2}. No significant changes in the size or shape of the ferricyanide redox wave were evident, in turn implying that the surface area of the electrode was not significantly altered by anodization (certainly not to an extent that would explain the increase in apparent current density seen in Figure 1 on its own). In contrast, a catalytic oxidation event highly suggestive of water oxidation seems to occur at a much lower onset potential after anodization than before (Figure S2, SI).

With no evidence to support an increase in surface area being the cause of the increased current density, and in light of our Tafel data suggesting that the nature of the electrode was radically altered, it seemed plausible that the electrodeposition of some species from solution onto the electrode could be the cause of the increased activity observed. This would also explain the slowly rising current after an initial lag phase observed in Figure 1. Accordingly, we analyzed anodized electrodes by SEM and EDX (Figure S4, SI). These results evinced no hints as to the presence of any surface deposits, suggesting that if any electrodeposition of catalytically active species had occurred, then the amounts deposited were very low. However, it was still possible that minute traces of impurities in the electrolyte were depositing onto the surface at very low levels. In this regard, we note that electrocatalytic water oxidation using ultralow loadings of cobalt were recently reported by Meyer and co-workers,[76] who were able to achieve a current density for water oxidation of 0.16 mA cm^{-2} at an overpotential of 0.8 V using phosphate buffer at pH 7.2 and loadings of cobalt on planar FTO as low as 7×10^{-11} mol/cm^2 (as judged by integration of cyclic voltammograms). Nocera and co-workers have also reported catalytic water oxidation at appreciable levels by heterogeneous cobalt oxides deposited from Co(II) impurities present in solutions of cobalt coordination complexes. In this study, the authors found that only 9×10^{-8} nmol of cobalt (in the form of heterogeneous cobalt oxyhydroxides) could give rise to current densities of 0.11 mA cm^{-2} (at ~0.9 V overpotential) at pH 7.[70] Hence, there is strong precedence for detectable and sustained water oxidation electrocatalysis in the presence of very small amounts of first-row transition-metal ions.

Accordingly, we altered our electrolyte and chose to probe sodium phosphate as an alternative buffer. Current densities were significantly lowered in this electrolyte at low and near-neutral pH, but more complete study of the overpotential required to achieve a current density of 1 mA cm^{-2} over the pH range 1−13 evinced an extraordinary shift at high pH to much lower values (see Figure 3). Indeed, we found that the

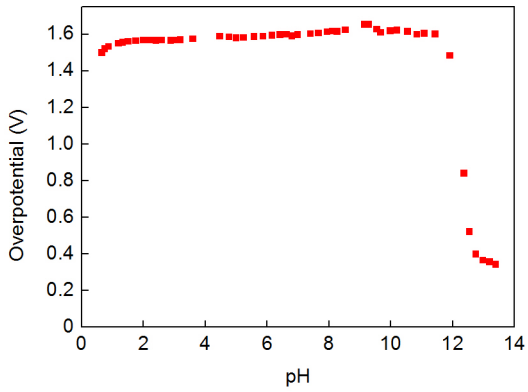

Figure 3. Galvanostatic overpotential vs pH profile (at a current density of 1 mA cm^{-2}) for an FTO working electrode (area = 1 cm^2) that had previously been anodized in 0.5 M potassium borate at pH 9.2 overnight at V = 1.2 V vs Ag/AgCl (R = 31.5 Ω). A Pt wire counter electrode and an Ag/AgCl reference electrode were used at room temperature. The overpotential required to achieve a current density of 1 mA cm^{-2} was then gauged when the voltage reading had stabilized (typically around 5 min after addition of each aliquot). The electrolyte for the galvanostatic experiment was initially 1 M H_3PO_4, to which aliquots of NaOH solution were added.

overpotential requirement was lowered to only 400 mV at pH 12.9 (for 1 mA cm^{-2}). Moreover, similar trends could be observed in 1 M sodium carbonate buffer (see Figures S5−S12, SI), suggesting that any impurity present in the electrolyte was possibly common to all these salts.

Some authors have suggested that tin oxide-based electrodes can undergo compositional changes when poised anodically in aqueous solutions, with a lowered overpotential for oxygen evolution and electrode corrosion manifesting as a result of an increase in the number of oxygen vacancies in the lattice.[77] In order to test whether this was a possible cause of the activity seen in the present case, we repeated the anodization procedure using a range of alternative substrates: commercial indium−tin oxide on glass (ITO), glassy carbon, boron-doped diamond, and platinum (see SI and Figures S5−S12). We also replaced our Pt counter electrode with carbon felt, in order to exclude the possibility of Pt leaching from the counter electrode and forming Pt oxides at the working electrode. Despite these changes, all combinations of substrate electrode and counter electrode that were examined displayed the familiar initial lag phase followed by a prolonged period of increase in current, resulting in final current densities between 4 and 1.5 mA cm^{-2} at overpotentials of between 540 and 660 mV (not corrected for resistance). These results seemed to rule out any changes in the structure or stoichiometry of the FTO electrode as the root cause of the high currents observed and eliminated Pt leached from the cathode as a source of activity.

We next repeated our standard anodization procedure in a two-compartment cell, where the working and counter electrodes were in different chambers separated by a Nafion membrane. The rationale behind this was to prevent any

DOI: 10.1021/jacs.5b08139
J. Am. Chem. Soc. 2015, 137, 13980−13988

impurities in solution from undergoing redox cycling between the anode and cathode. This division of the cell made no difference whatsoever to the rate of increase of the current density upon anodization and did not alter the final current density reached (Figure S10, SI). Likewise, rates of current density increase and peak current densities were again unaffected by changing the Pt counter electrode for a carbon cloth counter electrode in this two-chamber electrolysis cell.

Substituting the Ag/AgCl reference electrode for a Hg/HgO reference electrode (to exclude the possibility of trace silver acting as a water oxidation catalyst, as reported recently by some authors[78−80]) gave rates of current density increase and peak current densities similar to those seen with the Ag/AgCl reference electrode. Furthermore, experiments undertaken in a two-electrode configuration with an FTO working electrode and carbon felt counter electrode also showed the now familiar current density profiles (see Figure S11, SI). These results suggested that the nature of the reference electrode (if any) was not the cause of the currents observed.

The above experiments in two-chambered cells suggested that the currents were not caused by redox-cycling of species in solution. We had also observed that slow bubbling was evident at the working electrode when current densities exceeded ∼1 mA cm^{-2}. To determine if oxygen production would account for the observed currents, we analyzed the headspace of sealed, airtight cells containing an FTO working electrode by gas chromatography (see the SI for experimental details). In all, three separate sets of conditions were probed: sodium phosphate buffer with an Hg/HgO reference electrode at pH 13.0 and an overpotential for water oxidation of 580 mV (Figure 4), sodium phosphate buffer with an Ag/AgCl reference electrode at pH 12.9 and an overpotential for water oxidation of 540 mV (Figure S13), and potassium borate buffer with an Ag/AgCl reference electrode at pH 9.1 and an overpotential for water oxidation of 570 mV (Figure S14). All three sets of conditions showed that the currents observed were indeed due overwhelmingly to oxygen production, with Faradaic efficiencies for these processes being 95% ± 6% for sodium phosphate buffer with an Hg/HgO reference electrode at pH 13.0, 90% ± 3% for sodium phosphate buffer with an Ag/AgCl reference electrode at pH 12.9, and 94% ± 8% for potassium borate buffer with an Ag/AgCl reference electrode at pH 9.2.

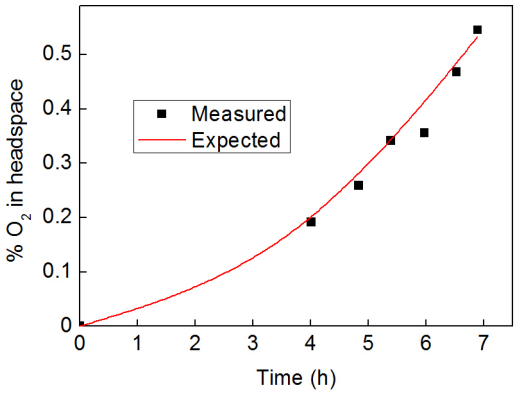

Figure 4. A representative trace showing gas chromatographic analysis of the headspace of an airtight cell during electrolysis of a solution of 0.5 M sodium phosphate at pH 13. An FTO working electrode, carbon felt counter electrode, and an Hg/HgO (1 M NaOH) reference electrode were used at an overpotential for water oxidation of 0.58 V (not corrected for resistance). The solid red line indicates the percent of oxygen expected in the cell headspace based on the charge passed during electrolysis (24 C in this case). Black squares indicate actual measurements of the percent of O_2 in the cell headspace as determined by gas chromatography.

With evidence to suggest that catalytic water oxidation was occurring, but still without firm evidence of the agent(s) responsible, we next turned our attention to analysis of our electrolyte solutions. Addition of the disodium salt of ethylenediaminetetraacetic acid (EDTA) to anodization reactions that were underway was observed to lead to a rapid and lasting reduction in current density (see Figure 5).

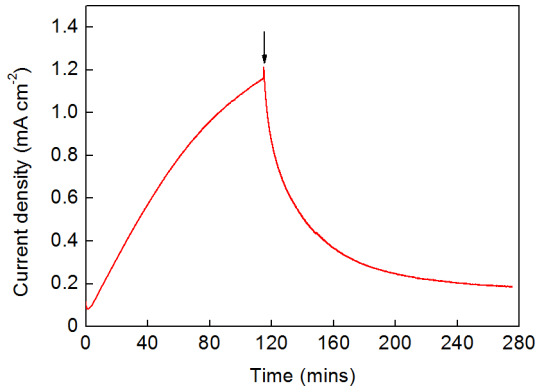

Figure 5. Bulk electrolysis with stirring of an aqueous solution of 0.5 M potassium borate (pH 9.2) on an FTO working electrode (area = 1 cm^2). A Pt wire counter electrode and an Ag/AgCl reference electrode were used at room temperature. An overpotential of 0.72 V was applied (not corrected for solution resistance, which was on the order of 40 Ω). After 114 min (indicated by the black arrow), around 20 mg of EDTA (sodium salt) was added as a solid.

This suggested that metal ions were indeed implicated in the water oxidation catalysis. However, our previous results mentioned above implied that these metal ions did not originate from any of the electrodes. Accordingly, we analyzed both fresh solutions and those that had previously supported anodization of electrodes by ICP-MS. This revealed relatively high (hundreds of ng to μg L^{-1}) levels of several transition metals to be present (including Fe, Ni, Mo, Cu, and Mn) in these buffer solutions, which were prepared with deionized water of 18.2 MΩ cm resistivity (see Table S1, SI).[81] In order to remove these metal ions from solution without introducing soluble agents (such as EDTA), which would remain in solution and potentially interfere with our analysis, we treated our buffer solutions with Amberlite IRC748 resin (an iminodiacetic acid chelating cation exchange resin for metal removal). In this way, it was hypothesized that any metal ions in the solution would be retained by the resin, which could then be separated from the electrolyte by filtration (see section SI-7 of the SI for experimental details).

Electrolysis experiments performed as before in such "washed" electrolytes did indeed evince significant attenuation in the rate of current density increase and a lowering of the peak current densities obtained (see Figure 6). Films that had been anodized in as-prepared electrolyte (until a steady current density had been reached) were subjected to analysis by CV in that electrolyte, and these CVs were compared to those obtained after the films had been removed from the as-prepared electrolyte and placed into electrolyte that had been washed

DOI: 10.1021/jacs.5b08139
J. Am. Chem. Soc. 2015, 137, 13980−13988

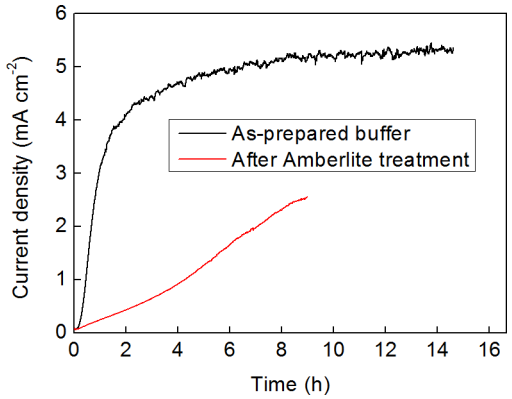

Figure 6. Comparison of electrolysis with and without pretreatment of the electrolyte with Amberlite (see procedure in section SI-7, SI). Red line: Bulk electrolysis with stirring of an aqueous solution of 0.5 M potassium borate (pH 9.2) that had previously been washed once with Amberlite IRC-748 resin. Black line: Bulk electrolysis with stirring of an aqueous solution of as-prepared 0.5 M potassium borate (pH 9.2) that had not previously been washed with Amberlite IRC-748 resin. In both cases, the working electrode was FTO (area = 1 cm^2). Single-compartment cells were used. Along with the FTO electrode, an Ag/AgCl reference electrode and a Pt wire counter electrode were employed. The experiments were performed at room temperature. An overpotential of 0.72 V was applied in each case (not corrected for solution resistance).

with Amberlite resin. CVs were recorded in the washed electrolyte every 5 min, with stirring of the electrolyte during the intervals. No bias was applied to the working electrode during these stirring periods. Figure S15 (SI) shows how the peak current that is obtained decays gradually over time under these conditions, implying that an electrode-bound deposit has indeed formed on the electrode during anodization (or else the current density obtained on moving to the washed electrolyte would be much lower from the outset). However, these results also suggest that this deposit is not stable when allowed to rest without applied bias in washed electrolyte solution with stirring.

When washed electrolytes were analyzed by ICP-MS and the concentrations of the various metal ions compared to those found in the electrolytes prior to washing with the Amberlite resin, only six metals were found to have significantly and consistently lower concentrations in the washed electrolytes (which gave correspondingly lower current densities) than in the as-prepared electrolytes: Pb, W, Mn, Mo, Ce, and Ni. Of these metals, Ni and Mn have previously been shown to display catalytic water oxidation activity under neutral and near-neutral conditions.[19−33] However, we re-examined all of these candidate metals for water oxidation activity by adding small amounts of various solids containing these ions to electrolysis experiments in 0.5 M sodium phosphate at pH 12.9 (see Figures S16−S21, SI). These experiments showed that Mo, W, and Ce salts had little or no effect on the trajectory of the current, while Mn actually caused the current density to diminish. Only Ni and Pb gave any increase in the current density above that which manifested in all such electrolyses.

Of these two metals, Ni seemed the more likely water oxidation catalyst for several reasons. First, Ni has already been shown to be a competent water oxidation catalyst by Nocera and co-workers, who were able to deposit thin (transparent) films of nickel oxides from 0.4 mM solutions of nickel salts.[22] These authors also noted an increase in current density of these films with anodization, which they attributed to structural changes in the nickel oxide film upon oxidation and a pH−overpotential profile highly reminiscent of that shown in Figure 3. Lead and its oxides, meanwhile, have been shown to give very high overpotentials for water oxidation,[82−84] and the oxides of lead tend to form red/brown anode deposits. The anodes in our anodization reactions were, by contrast, always transparent (see Figure S22, SI).

To confirm that Ni was indeed responsible for the water oxidation activity seen in the experiments described above, XPS (Al Kα source) was performed on FTO electrodes that had been subjected to electrolysis in as-prepared 0.5 M sodium phosphate (pH 12.9), as-prepared 0.5 M potassium borate (pH 9.2), and 0.5 M potassium borate (pH 9.2) that had previously been washed with Amberlite resin. A control FTO electrode that had not been subjected to any electrolysis was also analyzed. Although weak, signals characteristic of nickel hydroxide and/or nickel oxyhydroxide (a larger peak at 856 eV and a smaller, broader peak 863 eV corresponding to the $2p_{3/2}$ spectra of $Ni(OH)_2$ and the β- and γ-polymorphs of NiOOH)[85] were clearly visible on the electrodes used in unwashed buffers, while these peaks were absent from the control and washed-buffer electrodes (see Figures S23−S25, SI).

The presence of low levels of Fe (as low as 0.01%) in nickel oxide films has been shown by Corrigan to have an observable effect on the oxygen evolution overpotential shown by such films.[71] This work has recently been revisited by both Boettcher[72−74] and Bell and co-workers,[40,75] who have reported excellent water oxidation electrocatalysis metrics for Fe-doped nickel oxides, with current densities of 10 mA cm^{-2} being achieved at 336 mV overpotential with $Ni_{0.9}Fe_{0.1}O_x$ in 1 M KOH[72] and a similar effect manifesting in near-neutral borate solutions.[74] Given the presence of Fe in the electrolyte solutions used in this work (both as-prepared and after washing), it thus seemed likely that similar Fe-doping could be occurring in this case. In order to investigate this possibility further, we examined glassy carbon electrodes that had been anodized in both as-prepared and washed sodium phosphate buffer (0.5 M, pH 12.9) using a Mg Kα source. These changes in both substrate and X-ray source from the aforementioned XPS analyses were necessary in order to obtain spectra where the characteristic Fe 2p peaks at ∼707 and 720 eV would not be obscured by any interference from Sn (in the FTO substrates) or Ni LMM Auger peaks.[73] The results of this analysis are shown in Figure S26 (SI). No peaks that can be reliably assigned to Fe were observed; however, we note that the sensitivity of the Mg Kα X-ray source is not as high as that of the Al Kα source used previously. Hence, it is possible (perhaps even likely, given that ICP-MS suggests that significant Fe is present in the electrolytes investigated) that iron is present in these deposits, but at levels that are too low to be detected with the Mg source. It is interesting to note that washing the electrolyte with Amberlite resin removes Ni (and therefore reduces the peak current densities that are obtained), but it does not seem to decrease the amount of Fe in solution (see Table S1, SI). We note, however, that a single wash with Amberlite resin is generally insufficient to remove all the Ni from solution or to prevent the associated current density increase upon polarization [see Table S1 (SI) and Figure 6]. Hence, if Ni−Fe oxides are forming, it seems that the amount of nickel present in solution is a critical determinant of the water oxidation activity that is observed. This agrees with the results obtained by Corrigan and by Boettcher and co-workers,

DOI: 10.1021/jacs.5b08139
J. Am. Chem. Soc. 2015, 137, 13980−13988

which suggest that the most active catalysts are predominantly nickel oxides containing a few percent of iron oxides.[71−73]

ICP-MS analysis of the electrolytes had suggested a nickel concentration of around 1 μg L^{-1} in the as-prepared potassium borate buffer solutions. Washing with Amberlite resin should lower this concentration, and multiple successive washes should cause the concentration of nickel to fall even further. This is borne out by Figure 7, which shows the effect that up to three

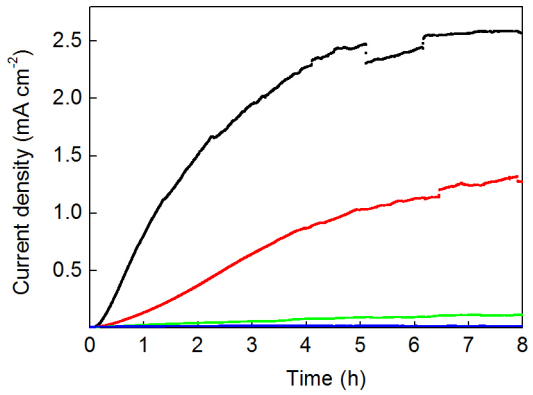

Figure 7. Bulk electrolysis experiments performed in 0.5 M sodium phosphate solution (pH 12.9), using an FTO working electrode (area = 1 cm^2), an Hg/HgO reference, and a Pt wire counter electrode. In all cases, an overpotential of 0.43 V (not corrected for resistance) was applied. The solutions had been subjected to washing with Amberlite resin to remove metal ion impurities as follows: black line, no washes (i.e., as prepared); red line, one wash; green line, two consecutive washes; blue line, three consecutive washes.

washing cycles have on the rate of current density increase and the peak current density that is obtained. Starting in as-prepared 0.5 M sodium phosphate solution at pH 12.9, ICP-MS gave a nickel concentration of 500 ± 20 ng L^{-1} and bulk electrolysis in this solution produced a current density of 2.6 mA cm^{-2} after 8 h (Figure 7, black trace). The current density fell after one wash with Amberlite resin to around 1.3 mA cm^{-2} after 8 h (red line) and to only 0.1 mA cm^{-2} after 8 h following two washes (green line). ICP-MS suggested that the nickel content of these washed solutions was 250 ± 10 and 200 ± 8 ng L^{-1}, respectively. After three washes, the current density barely rose at all over the 8 h period of electrolysis, reaching only 0.02 mA cm^{-2} after this time (Figure 7, blue line), and reliable values for the concentration of nickel in this solution could not be obtained by ICP-MS, possibly as the levels of nickel present were too low. These results suggest that iterative removal of the nickel present in solution causes an iterative decrease in the rate at which the current density increases and the maximum current density that can be achieved within a certain time window. In conjunction with the electrochemical and XPS data, this again implies that nickel is a cause of the water oxidation activity observed.

A nickel concentration in solution of 1 μg L^{-1} corresponds to around 3.4×10^{-10} mol of nickel ions present in the 20 mL of electrolyte typically used in the electrolysis experiments described in this report. This in turn equates to a nickel concentration of ∼17 nM, or over 23 000 times less nickel than that used by Nocera and co-workers when depositing their ultrathin nickel oxide films.[22] We note, however, that if the explicit intention is to deposit a nickel oxide film for water oxidation, then the concentrations used in such earlier reports are likely to be more effective; our interest here merely extends to showing that 17 nM solutions of nickel *can* give rise to catalysis, and we do not claim that films deposited at these lower concentrations of nickel give superior (or even comparable) performance to films deposited from more concentrated solutions.

Assuming that all the nickel present in the electrolyte becomes deposited on the working electrode during electrolysis (and this is a significant overestimate of the amount of Ni that is deposited, as "used" solutions are still capable of causing fresh working electrodes to become activated in this way), then a *maximum* coverage of about 0.34 nmol cm^{-2} of nickel is obtained, or approximately one close-packed monolayer.[76] This is about 10 000 times lower loading of nickel than reported recently by Zhang and co-workers[24] and ∼20 times lower loading than that reported by Nocera and co-workers for their ultrathin films. As the actual coverage in our case may be significantly less than one monolayer, this might also explain why the Tafel slopes obtained for anodized films in this work are somewhat higher than those previously reported.[23]

CONCLUSIONS

Herein, we have shown that loadings of nickel of below 1 nmol per cm^2 are effective for water oxidation across the pH range 9.2−13, displaying an overpotential requirement of 400 mV in order to achieve a current density of 1 mA cm^{-2} at pH 13. These are very low loadings of nickel, and indeed (as in our own case), such small amounts of nickel can be found in many common electrolyte salts. It is also possible that adventitious iron is codepositing with nickel to produce highly active water oxidation catalysts. However, it appears that the amount of nickel present in solution is a critical determinant of catalytic activity, inasmuch as removal of Ni leads to a reduction in catalytic current despite high levels of Fe remaining in solution. In view of the number of investigators undertaking similar work in this field, it is thus essential that the agency of trace metal ions, and nickel in particular, is excluded from any future reports of water oxidation catalysis within the pH range 9.2−13. It also remains critical that the nature of the true catalyst performing water oxidation is firmly established in all cases,[69,70] noting that catalysis can manifest from extremely low levels of impurities.[65] This must be held to be especially true in cases where the measured activity for water oxidation is comparable to or below that reported in this paper. In these cases, ever more rigorous control experiments must be performed in order to demonstrate genuine catalysis by the species under consideration.

EXPERIMENTAL SECTION

Materials. Nickel(II) hexahydrate (99.997%), potassium ferricyanide(III), potassium hydroxide (90%), sodium hydroxide (98−100.5%), sodium phosphate dibasic (98.5%), potassium nitrate (90%), sodium carbonate (99.95−100%), and ethylenediaminetetraacetic acid (sodium salt) were purchased from Sigma-Aldrich; 0.180 mm-thick Nafion N-118 membrane, boric acid 99.99%, Amberlite IRC-748, and phosphoric acid (85%) were supplied by Alfa Aesar. All chemical reagents and solvents were used as purchased, except the Amberlite resin, which was stirred for 45 min in ultrapure water and filtered before use, in order to remove any nonbound chelating agent from the beads (see also section SI-7, SI).

All electrolyte solutions were prepared with reagent-grade water (18.2 MΩ cm resistivity), obtained from a Sartorius Arium Comfort combined water system. pH determinations were made with a Hanna HI 9124 waterproof pH meter. UV−vis spectra were collected in the

DOI: 10.1021/jacs.5b08139
J. Am. Chem. Soc. 2015, 137, 13980−13988

solid state on a JASCO V-670 spectrophotometer. FTO-coated plain float electrodes (7 Ω per sheet) were purchased from Hartford Glass Co., Inc. ITO-coated plain float electrodes (12−15 Ω per square) were purchased from Optical Filters. All other materials were obtained as stated in the text. Experiments performed at "room temperature" were carried out at 20 °C.

Electrochemical studies were performed in a three-electrode configuration (unless otherwise stated) using both CH Instruments CHI760D potentiostats and Biologic SP-150 potentiostats. A Pt wire was used as the counter electrode (unless otherwise stated), and either an Ag/AgCl (NaCl, 3 M) reference electrode (RE 5B, BASi) or an Hg/HgO (1 M NaOH) reference electrode (CH Instruments CHI-152) was used as the reference electrode as specified. Working electrodes were washed with acetone and deionized water prior to use. Pt wire was washed with HCl and rinsed in water after every experiment to remove any metal that may have deposited on its surface. Carbon felt counter electrodes were not reused. Three-electrode potentials were converted to the NHE reference scale using $E(\mathrm{NHE}) = E(\mathrm{Ag/AgCl}) + 0.209$ V and $E(\mathrm{NHE}) = E(\mathrm{Hg/HgO}) + 0.098$ V. Unless otherwise stated, the active area of all FTO and ITO electrodes was set to 1 cm^2.

Bulk Electrolysis and in Situ Catalyst Formation. Bulk electrolyses were performed in a three-electrode configuration (unless otherwise stated) in both single- and two-compartment electrochemical cells. In the latter case, the compartments of the H-cell were separated by a 0.180-mm-thick Nafion N-118 membrane, with this membrane being held in place by judicious application of Araldite epoxy glue (Bostik Findley, Ltd., UK). Solutions were stirred, the same stirring rate being kept for all experiments. Where voltages have been corrected for ohmic resistances, the effective voltage ($V_{\mathrm{effective}}$) is given by[86]

$$V_{\mathrm{effective}} = V_{\mathrm{applied}} - iR$$

where i is the current flowing through the cell and R is the resistance of the cell. Cell resistances were measured by the iR test function available on the CH potentiostats, using the general method developed by He and Faulkner.[87] Briefly, the iR test function works by examining the current response to small step changes in voltage relative to a test potential at which no Faradaic current flows. In our case, the step change (ΔV) was 0.05 V and the test potential was selected as 0 V vs Ag/AgCl. Other test voltages over the range from 0 to 1 V vs Ag/AgCl gave answers for the solution resistance that were within error of the values obtained at 0 V. The iR test function on the potentiostat then extrapolates the signal-averaged currents at 54 and 72 ps after the voltage-step edge backward to obtain a current at $t = 0$, where this current can also be expressed as $\Delta V/R$. R in this case is the solution resistance that is sought. The final parameter that the user must select with this function is the acceptable stability limit of the system at the value of R measured ("% overshoot"): in our case a value of 2% was chosen (default setting on the potentiostat). The error associated with this iR correction is dominated by the error associated with gauging the resistance of the solution, where values were found to vary over a range of $R_{\mathrm{measured}} \pm 3\%$. Resistances could be automatically compensated on the biologic potentiostats, using the ZIR function.

Details of specific experimental configurations and other methods and materials are given in the SI.

■ ASSOCIATED CONTENT

Supporting Information

The Supporting Information is available free of charge on the ACS Publications website at DOI: 10.1021/jacs.5b08139.

Experimental protocols, additional electrochemical data, details of gas analysis, and structural and spectroscopic characterization of electrodes (PDF)

■ AUTHOR INFORMATION

Corresponding Author

*mark.symes@glasgow.ac.uk

Author Contributions

The manuscript was written through contributions of both authors.

Notes

The authors declare no competing financial interest.

■ ACKNOWLEDGMENTS

M.D.S. thanks the University of Glasgow for a Kelvin Smith Research Fellowship. This work was supported by the University of Glasgow and an EPSRC (UK) Small Equipment Grant to M.D.S. (grant number EP/K031732/1). The data which underpin this work are available at http://dx.doi.org/10.5525/gla.researchdata.227 ("Efficient Electrocatalytic Water Oxidation at Neutral and High pH by Adventitious Nickel at Nanomolar Concentrations") and are licensed as CC BY-SA 4.0. We thank Alexander Clunie (University of Strathclyde) for ICP-MS measurements, Jim Gallagher (University of Glasgow) for assistance with the SEM measurements, and Prof. Leroy Cronin and the Glasgow Solar Fuels network (University of Glasgow) for use of shared facilities. X-ray photoelectron spectra were obtained at the National EPSRC XPS Users' Service (NEXUS) at Newcastle University, an EPSRC Mid-Range Facility.

■ REFERENCES

(1) Lewis, N. S.; Nocera, D. G. *Proc. Natl. Acad. Sci. U. S. A.* **2006**, *103*, 15729.
(2) Tachibana, Y.; Vayssieres, L.; Durrant, J. R. *Nat. Photonics* **2012**, *6*, 511.
(3) Dasgupta, S.; Brunschwig, B. S.; Winkler, J. R.; Gray, H. B. *Chem. Soc. Rev.* **2013**, *42*, 2213.
(4) Carmo, M.; Fritz, D. L.; Mergel, J.; Stolten, D. *Int. J. Hydrogen Energy* **2013**, *38*, 4901.
(5) Holladay, J. D.; Hu, J.; King, D. L.; Wang, Y. *Catal. Today* **2009**, *139*, 244.
(6) Cook, T. R.; Dogutan, D. K.; Reece, S. Y.; Surendranath, Y.; Teets, T. S.; Nocera, D. G. *Chem. Rev.* **2010**, *110*, 6474.
(7) Pletcher, D.; Li, X. *Int. J. Hydrogen Energy* **2011**, *36*, 15089.
(8) McKone, J. R.; Lewis, N. S.; Gray, H. B. *Chem. Mater.* **2014**, *26*, 407.
(9) Symes, M. D.; Cronin, L. Materials for Water Splitting. In *Materials for a Sustainable Future*; RSC Publishing: Cambridge (UK), 2012; pp 592−614.
(10) Kanan, M. W.; Nocera, D. G. *Science* **2008**, *321*, 1072.
(11) Lutterman, D. A.; Surendranath, Y.; Nocera, D. G. *J. Am. Chem. Soc.* **2009**, *131*, 3838.
(12) Kanan, M. W.; Surendranath, Y.; Nocera, D. G. *Chem. Soc. Rev.* **2009**, *38*, 109.
(13) Gerken, J. B.; Landis, E. C.; Hamers, R. J.; Stahl, S. S. *ChemSusChem* **2010**, *3*, 1176.
(14) Gerken, J. B.; McAlpin, J. G.; Chen, J. Y. C.; Rigsby, M. L.; Casey, W. H.; Britt, R. D.; Stahl, S. S. *J. Am. Chem. Soc.* **2011**, *133*, 14431.
(15) Cobo, S.; Heidkamp, J.; Jacques, P.-A.; Fize, J.; Fourmond, V.; Guetaz, L.; Jousselme, B.; Ivanova, V.; Dau, H.; Palacin, S.; Fontecave, M.; Artero, V. *Nat. Mater.* **2012**, *11*, 802.
(16) Bloor, L. G.; Molina, P. I.; Symes, M. D.; Cronin, L. *J. Am. Chem. Soc.* **2014**, *136*, 3304.
(17) Risch, M.; Ringleb, F.; Kohlhoff, M.; Bogdanoff, P.; Chernev, P.; Zaharieva, I.; Dau, H. *Energy Environ. Sci.* **2015**, *8*, 661.
(18) Hutchings, G. S.; Zhang, Y.; Li, J.; Yonemoto, B. T.; Zhou, X.; Zhu, K.; Jiao, F. *J. Am. Chem. Soc.* **2015**, *137*, 4223.

DOI: 10.1021/jacs.5b08139
J. Am. Chem. Soc. 2015, 137, 13980−13988

(19) Dincă, M.; Surendranath, Y.; Nocera, D. G. *Proc. Natl. Acad. Sci. U. S. A.* **2010**, *107*, 10337.
(20) Risch, M.; Klingan, K.; Heidkamp, J.; Ehrenberg, D.; Chernev, P.; Zaharieva, I.; Dau, H. *Chem. Commun.* **2011**, *47*, 11912.
(21) Singh, A.; Chang, S.; Hocking, R. K.; Bach, U.; Spiccia, L. *Energy Environ. Sci.* **2013**, *6*, 579.
(22) Bediako, D. K.; Lassalle-Kaiser, B.; Surendranath, Y.; Yano, J.; Yachandra, V. K.; Nocera, D. G. *J. Am. Chem. Soc.* **2012**, *134*, 6801.
(23) Bediako, D. K.; Surendranath, Y.; Nocera, D. G. *J. Am. Chem. Soc.* **2013**, *135*, 3662.
(24) Wang, J.; Li, K.; Zhong, H.-X.; Xu, D.; Wang, Z.-L.; Jiang, Z.; Wu, Z.-J.; Zhang, X.-B. *Angew. Chem., Int. Ed.* **2015**, *54*, 10530.
(25) Jiao, F.; Frei, H. *Chem. Commun.* **2010**, *46*, 2920.
(26) Gorlin, Y.; Jaramillo, T. F. *J. Am. Chem. Soc.* **2010**, *132*, 13612.
(27) Zaharieva, I.; Chernev, P.; Risch, M.; Klingan, K.; Kohlhoff, M.; Fischer, A.; Dau, H. *Energy Environ. Sci.* **2012**, *5*, 7081.
(28) Izgorodin, A.; Izgorodina, E.; MacFarlane, D. R. *Energy Environ. Sci.* **2012**, *5*, 9496.
(29) Najafpour, M. M.; Ehrenberg, T.; Wiechen, M.; Kurz, P. *Angew. Chem., Int. Ed.* **2010**, *49*, 2233.
(30) Takashima, T.; Hashimoto, K.; Nakamura, R. *J. Am. Chem. Soc.* **2012**, *134*, 1519.
(31) Takashima, T.; Hashimoto, K.; Nakamura, R. *J. Am. Chem. Soc.* **2012**, *134*, 18153.
(32) Indra, A.; Menezes, P. W.; Zaharieva, I.; Baktash, E.; Pfrommer, J.; Schwarze, M.; Dau, H.; Driess, M. *Angew. Chem., Int. Ed.* **2013**, *52*, 13206.
(33) Jin, K.; Park, J.; Lee, J.; Yang, K. D.; Pradhan, G. K.; Sim, U.; Jeong, D.; Jang, H. L.; Park, S.; Kim, D.; Sung, N.-E.; Kim, S. H.; Han, S.; Nam, K. T. *J. Am. Chem. Soc.* **2014**, *136*, 7435.
(34) Du, J.; Chen, Z.; Ye, S.; Wiley, B. J.; Meyer, T. J. *Angew. Chem., Int. Ed.* **2015**, *54*, 2073.
(35) Yu, F.; Li, F.; Zhang, B.; Li, H.; Sun, L. *ACS Catal.* **2015**, *5*, 627.
(36) Li, T.-T.; Cao, S.; Yang, C.; Chen, Y.; Lv, X.-J.; Fu, W.-F. *Inorg. Chem.* **2015**, *54*, 3061.
(37) Smith, R. D. L.; Prévot, M. S.; Fagan, R. D.; Zhang, Z.; Sedach, P. A.; Siu, M. K. J.; Trudel, S.; Berlinguette, C. P. *Science* **2013**, *340*, 60.
(38) Smith, R. D. L.; Prévot, M. S.; Fagan, R. D.; Trudel, S.; Berlinguette, C. P. *J. Am. Chem. Soc.* **2013**, *135*, 11580.
(39) Gong, M.; Li, Y.; Wang, H.; Liang, Y.; Wu, J. Z.; Zhou, J.; Wang, J.; Regier, T.; Wei, F.; Dai, H. *J. Am. Chem. Soc.* **2013**, *135*, 8452.
(40) Friebel, D.; Louie, M. W.; Bajdich, M.; Sanwald, K. E.; Cai, Y.; Wise, A. M.; Cheng, M.-J.; Sokaras, D.; Weng, T.-C.; Alonso-Mori, R.; Davis, R. C.; Bargar, J. R.; Nørskov, J. K.; Nilsson, A.; Bell, A. T. *J. Am. Chem. Soc.* **2015**, *137*, 1305.
(41) Burke, M. S.; Kast, M. G.; Trotochaud, L.; Smith, A. M.; Boettcher, S. W. *J. Am. Chem. Soc.* **2015**, *137*, 3638.
(42) Hunter, B. M.; Blakemore, J. D.; Deimund, M.; Gray, H. B.; Winkler, J. R.; Müller, A. M. *J. Am. Chem. Soc.* **2014**, *136*, 13118.
(43) Fominykh, K.; Chernev, P.; Zaharieva, I.; Sicklinger, J.; Stefanic, G.; Döblinger, M.; Müller, A.; Pokharel, A.; Böcklein, S.; Scheu, C.; Bein, T.; Fattakhova-Rohlfing, D. *ACS Nano* **2015**, *9*, 5180.
(44) Cady, C. W.; Gardner, G.; Maron, Z. O.; Retuerto, M.; Go, Y. B.; Segan, S.; Greenblatt, M.; Dismukes, G. C. *ACS Catal.* **2015**, *5*, 3403.
(45) Zhong, D. K.; Sun, J.; Inumaru, H.; Gamelin, D. R. *J. Am. Chem. Soc.* **2009**, *131*, 6086.
(46) Reece, S. Y.; Hamel, J. A.; Sung, K.; Jarvi, T. D.; Esswein, A. J.; Pijpers, J. J. H.; Nocera, D. G. *Science* **2011**, *334*, 645.
(47) Barroso, M.; Cowan, A. J.; Pendlebury, S. R.; Grätzel, M.; Klug, D. R.; Durrant, J. R. *J. Am. Chem. Soc.* **2011**, *133*, 14868.
(48) Seabold, J. A.; Choi, K.-S. *Chem. Mater.* **2011**, *23*, 1105.
(49) Yang, J.; Walczak, K.; Anzenberg, E.; Toma, F. M.; Yuan, G.; Beeman, J.; Schwartzberg, A.; Lin, Y.; Hettick, M.; Javey, A.; Ager, J. W.; Yano, J.; Frei, H.; Sharp, I. D. *J. Am. Chem. Soc.* **2014**, *136*, 6191.
(50) Li, R.; Chen, Z.; Zhao, W.; Zhang, F.; Maeda, K.; Huang, B.; Shen, S.; Domen, K.; Li, C. *J. Phys. Chem. C* **2013**, *117*, 376.
(51) Eisenberg, D.; Ahn, H. S.; Bard, A. J. *J. Am. Chem. Soc.* **2014**, *136*, 14011.
(52) Kenney, M. J.; Gong, M.; Li, Y.; Wu, J. Z.; Feng, J.; Lanza, M.; Dai, H. *Science* **2013**, *342*, 836.
(53) Sun, K.; McDowell, M. T.; Nielander, A. C.; Hu, S.; Shaner, M. R.; Yang, F.; Brunschwig, B. S.; Lewis, N. S. *J. Phys. Chem. Lett.* **2015**, *6*, 592.
(54) Abdi, F. F.; Han, L.; Smets, A. H. M.; Zeman, M.; Dam, B.; van de Krol, R. *Nat. Commun.* **2013**, *4*, 2195.
(55) Sun, K.; Saadi, F. H.; Lichterman, M. F.; Hale, W. G.; Wang, H.-P.; Zhou, X.; Plymale, N. T.; Omelchenko, S. T.; He, J.-H.; Papadantonakis, K. M.; Brunschwig, B. S.; Lewis, N. S. *Proc. Natl. Acad. Sci. U. S. A.* **2015**, *112*, 3612.
(56) Harriman, A.; Pickering, I. J.; Thomas, J. M.; Christensen, P. A. *J. Chem. Soc., Faraday Trans. 1* **1988**, *84*, 2795.
(57) Tsuji, E.; Imanishi, A.; Fukui, K.-i.; Nakato, Y. *Electrochim. Acta* **2011**, *56*, 2009.
(58) Ouattara, L.; Fierro, S.; Frey, O.; Koudelka, M.; Comninellis, C. *J. Appl. Electrochem.* **2009**, *39*, 1361.
(59) Tilley, S. D.; Cornuz, M.; Sivula, K.; Grätzel, M. *Angew. Chem., Int. Ed.* **2010**, *49*, 6405.
(60) Schley, N. D.; Blakemore, J. D.; Subbaiyan, N. K.; Incarvito, C. D.; D'Souza, F.; Crabtree, R. H.; Brudvig, G. W. *J. Am. Chem. Soc.* **2011**, *133*, 10473.
(61) Blakemore, J. D.; Mara, M. W.; Kushner-Lenhoff, M. N.; Schley, N. D.; Konezny, S. J.; Rivalta, I.; Negre, C. F. A.; Snoeberger, R. C.; Kokhan, O.; Huang, J.; Stickrath, A.; Tran, L. A.; Parr, M. L.; Chen, L. X.; Tiede, D. M.; Batista, V. S.; Crabtree, R. H.; Brudvig, G. W. *Inorg. Chem.* **2013**, *52*, 1860.
(62) Minguzzi, A.; Lugaresi, O.; Achilli, E.; Locatelli, C.; Vertova, A.; Ghigna, P.; Rondinini, S. *Chem. Sci.* **2014**, *5*, 3591.
(63) McCrory, C. C. L.; Jung, S.; Ferrer, I. M.; Chatman, S. M.; Peters, J. C.; Jaramillo, T. F. *J. Am. Chem. Soc.* **2015**, *137*, 4347.
(64) Widegren, J. A.; Finke, R. G. *J. Mol. Catal. A: Chem.* **2003**, *198*, 317.
(65) Crabtree, R. H. *Chem. Rev.* **2012**, *112*, 1536.
(66) Artero, V.; Fontecave, M. *Chem. Soc. Rev.* **2013**, *42*, 2338.
(67) Fukuzumi, S.; Hong, D. *Eur. J. Inorg. Chem.* **2014**, *2014*, 645.
(68) Stracke, J. J.; Finke, R. G. *J. Am. Chem. Soc.* **2011**, *133*, 14872.
(69) Stracke, J. J.; Finke, R. G. *ACS Catal.* **2014**, *4*, 909.
(70) Ullman, A. M.; Liu, Y.; Huynh, M.; Bediako, D. K.; Wang, H.; Anderson, B. L.; Powers, D. C.; Breen, J. J.; Abruña, H. D.; Nocera, D. G. *J. Am. Chem. Soc.* **2014**, *136*, 17681.
(71) Corrigan, D. A. *J. Electrochem. Soc.* **1987**, *134*, 377.
(72) Trotochaud, L.; Ranney, J. K.; Williams, K. N.; Boettcher, S. W. *J. Am. Chem. Soc.* **2012**, *134*, 17253.
(73) Trotochaud, L.; Young, S. L.; Ranney, J. K.; Boettcher, S. W. *J. Am. Chem. Soc.* **2014**, *136*, 6744.
(74) Smith, A. M.; Trotochaud, L.; Burke, M. S.; Boettcher, S. W. *Chem. Commun.* **2015**, *51*, 5261.
(75) Louie, M. W.; Bell, A. T. *J. Am. Chem. Soc.* **2013**, *135*, 12329.
(76) Kent, C. A.; Concepcion, J. J.; Dares, C. J.; Torelli, D. A.; Rieth, A. J.; Miller, A. S.; Hoertz, P. G.; Meyer, T. J. *J. Am. Chem. Soc.* **2013**, *135*, 8432.
(77) Kraft, A.; Hennig, H.; Herbst, A.; Heckner, K.-H. *J. Electroanal. Chem.* **1994**, *365*, 191.
(78) Wang, W.; Zhao, Q.; Dong, J.; Li, J. *Int. J. Hydrogen Energy* **2011**, *36*, 7374.
(79) Zhao, Q.; Yu, Z.; Hao, G.; Yuan, W.; Li, J. *Int. J. Hydrogen Energy* **2014**, *39*, 1364.
(80) Du, J.; Chen, Z.; Chen, C.; Meyer, T. J. *J. Am. Chem. Soc.* **2015**, *137*, 3193.
(81) The main metal impurities in the deionized water itself (which should contain between 30 and 40 μg/L total dissolved solids on the basis of a resistivity of 18.2 MΩ cm) appear to be Na, K, and Ca (see Table S1, SI), although low ng/L levels of other impurities cannot be ruled out.
(82) Ho, J. C. K.; Tremiliosi Filho, G.; Simpraga, R.; Conway, B. E. *J. Electroanal. Chem.* **1994**, *366*, 147.
(83) Amadelli, R.; Maldotti, A.; Molinari, A.; Danilov, F. I.; Velichenko, A. B. *J. Electroanal. Chem.* **2002**, *534*, 1.

DOI: 10.1021/jacs.5b08139
J. Am. Chem. Soc. 2015, 137, 13980−13988

(84) Sirés, I.; Low, C. T. J.; Ponce-de-León, C.; Walsh, F. C. *Electrochim. Acta* **2010**, *55*, 2163.
(85) Grosvenor, A. P.; Biesinger, M. C.; Smart, R. St.C.; McIntyre, N. S. *Surf. Sci.* **2006**, *600*, 1771.
(86) Hamann, C. H.; Hamnett, A.; Vielstich, W. *Electrochemistry*, 2nd ed.; Wiley-VCH, Weinheim, 2007.
(87) He, P.; Faulkner, L. R. *Anal. Chem.* **1986**, *58*, 517.

DOI: 10.1021/jacs.5b08139
J. Am. Chem. Soc. 2015, 137, 13980−13988